Anchor Selection in Angle-of-Arrival estimation-based localization using Polynomial Chaos Expansions

Thomas Van der Vorst[1,2], Trung-Hien Nguyen[1], Shaghayegh Monfared[1], Aziz Benlarbi-Delaï[2], Julien Sarrazin[2], François Horlin[1], Philippe De Doncker[1]
[1]Université libre de Bruxelles (ULB), Av. Roosevelt 50, 1050 Brussels, Belgium
[2] Sorbonne Université, L2E, UR2, F-75005 Paris, France
Contact : tvdvorst@ulb.ac.be

***Abstract*—Angle-of-arrival (AoA) estimation-based localization systems are a promising technology in the context of Internet-of-Things. The system considered is a densely deployed set of anchors equipped with arrays of antennas able to measure the AoA of the signal emitted by the device to be located. Naturally, the AoA measurements are prone to uncertainties due to noise, channel conditions and uncertainties on the anchors placement and orientations. In this work, a method based on Polynomial Chaos Expansions is proposed to perform anchor selection in order to enhance the precision of the positioning. An experimental setup with six anchors is implemented to evaluate the performance of the proposed method. The experimental results demonstrate that by applying our anchor selection method, the performance of the localization system improves.**

***Index Terms*—localization, anchor selection, polynomial chaos expansions, uncertainty**

I. Introduction

The development of wireless telecommunication systems, as well as the emergence of the 5G network have led to a gigantic increase of the number of devices connected to the network: the so-called Internet-of-Things. Many applications of those devices will require precise positioning [1]. For instance industrial process automation including asset tracking, or industrial control such as robot positioning applications may require a localization accuracy within 10 cm [2]. Many applications of the 5G network outside the IoT framework will also benefit from enhanced positioning capabilities. Improving the localization or positioning accuracy is therefore an important topic to address nowadays.

Angle-of-arrival (AoA) estimation-based localization is a promising technology for narrowband IoT applications that need precise positioning, especially in indoor scenarios. It requires a set of anchors of known position able to measure the AoA of the signal emitted by the device to be located. These anchors are therefore equipped with an array of antennas. To the best of our knowledge, none of the AoA estimation-based localization methods present in the literature provides simultaneously the position estimate with an uncertainty indicator on this position. However for some applications, it is crucial to know whether the position estimate is reliable or not.

In our previous work, a method based on Polynomial Chaos Expansions (PCE) was introduced to obtain confidence regions around the estimated position [3], [4]. These confidence regions can serve as uncertainty indicators associated with each position estimation.

In this work a localization system formed by a densely deployed network of anchors is considered. As more anchors than needed for localization are available in those conditions, anchor selection is a possibility to enhance the precision of the positioning. Anchor selection for AoA localization in the literature mostly concerns acoustic sensors [5], and do not rely on the uncertainty of AoA measurements. Instead, methods of outlier detection that are able to detect if one of the measurements is strongly biased are proposed [6]. In fact the uncertainty on the AoA measurement can be modelled as a sum of two effects: the measurement noise, which can be modelled as a Gaussian distribution around the true AoA, and outlier measurements which can be modelled as a Uniform distributed random variable [7]. This work focuses on the first type of uncertainty.

We propose an anchor selection method based on sensitivity indices obtained using the PCE framework. We assembled an experimental setup with six anchors using Universal Software Radio Peripheral (USRP). We demonstrated the performance of our localization method by applying it on measurements collected with the experimental setup. This paper is organized as follows: section II explains our method for anchor selection in AoA localization using PCE. Section III presents the experimental setup used for the measurements. Section IV presents some results and discusses the performance of our method, before concluding the article.

II. Method

A. AoA estimation-based localization

Consider the scenario where an emitting device of unknown position $\mathbf{x} = (\mathrm{x}, \mathrm{y})$ is to be located by a set of N anchors of known positions $\mathbf{x}_i = (\mathrm{x}_i, \mathrm{y}_i)$. This device is transmitting a signal in order to communicate. The positioning process is composed of two distinct steps. First, every anchor measures the AoA of the signal emitted by the device. Then, at a central

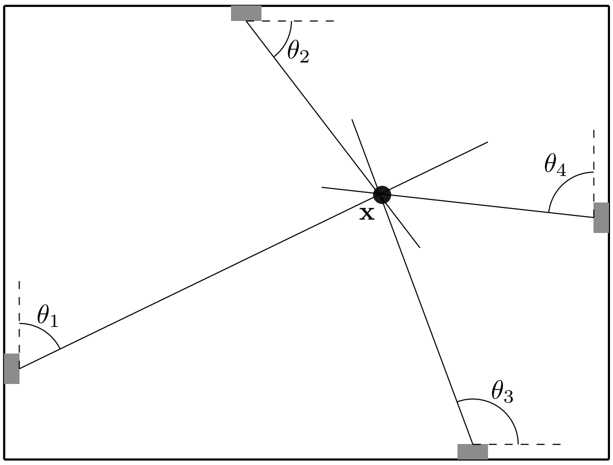

Fig. 1. Generic scenario for AoA estimation-based localization. Four anchors are represented by grey rectangles. An IoT device to be located is represented by a black dot. From the signal emitted by the device, each anchor estimates the AoA θ_i of the signal. The intersection of the bearing lines defined by these AoA's allows one to estimate the position of the device.

computer, the position of the device is estimated from all the AoA measurements associated with the known position of the anchors. An illustration of this general situation is given in Fig. 1.

The anchors are equipped with antenna arrays. The AoA of the signal is obtained by analysing the phase difference between the received signal at each antenna. Common methods to compute the AoA include Beamforming [9] or multiple signal classification (MUSIC) [10]. The AoA measured at anchor i, θ_i is subject to a measurement error n_i:

$$\theta_i = \arctan\left(\frac{\mathrm{y} - \mathrm{y}_i}{\mathrm{x} - \mathrm{x}_i}\right) + n_i \qquad i = 1, ..., N \tag{1}$$

Throughout this work, the errors n_i are assumed to be independent, zero-mean white Gaussian distributed random variables of variance $\sigma^2_{\theta_i}$.

The linear least-squares estimator gives an estimation of the device position $\hat{\boldsymbol{x}} = (\hat{x}, \hat{y})$ using the anchors locations and the AoA measurements as [8]:

$$\hat{\boldsymbol{x}} = (\mathbf{H}^T\mathbf{H})^{-1}\mathbf{H}^T\mathbf{b} \tag{2}$$

where

$$\mathbf{H} = \begin{bmatrix} \tan\theta_1 & -1 \\ \tan\theta_2 & -1 \\ \vdots & \vdots \\ \tan\theta_N & -1 \end{bmatrix} \tag{3}$$

and

$$\mathbf{b} = \begin{bmatrix} \mathrm{x}_1 \tan\theta_1 - \mathrm{y}_1 \\ \mathrm{x}_2 \tan\theta_2 - \mathrm{y}_2 \\ \vdots \\ \mathrm{x}_N \tan\theta_N - \mathrm{y}_N \end{bmatrix}. \tag{4}$$

In the case of two-dimension localization problem, a minimum of two anchors is needed.

B. Polynomial Chaos Expansions of the position

The interest of the Polynomial Chaos Expansion theory is to obtain statistical informations on the model response with less computational effort than by a Monte-Carlo simulation of the actual model. The estimation of the x- and y-coordinates are separately expanded on the same polynomial chaos basis [4]:

$$\hat{x} = \sum_{\boldsymbol{\alpha} \in \mathcal{A}} d_{\boldsymbol{\alpha}} \Psi_{\boldsymbol{\alpha}}(\{\theta_i\}_{i=1}^N) \tag{5}$$

$$\hat{y} = \sum_{\boldsymbol{\alpha} \in \mathcal{A}} e_{\boldsymbol{\alpha}} \Psi_{\boldsymbol{\alpha}}(\{\theta_i\}_{i=1}^N). \tag{6}$$

In those equations, $d_{\boldsymbol{\alpha}}$ and $e_{\boldsymbol{\alpha}}$ are the coefficients of the expansion of the estimates of the x- and y-coordinates, respectively. The multi-indices $\boldsymbol{\alpha}$ give the degree of the used polynomials. The set of indices $\mathcal{A}$ is determined by the parameters of the expansions: the number of variables and the total degree of the expansion. Detailed explanations on the PCE and the way to compute the coefficients can be found in [4]. It can be easily demonstrated that the mean and the variance of the x-coordinate are respectively given by:

$$\mu_{\hat{x}} = \mathbb{E}[\hat{x}] = d_{\mathbf{0}} \tag{7}$$

$$\sigma^2_{\hat{\boldsymbol{x}}} = \mathrm{Var}\left[\sum_{\boldsymbol{\alpha} \in \mathcal{A}} d_{\boldsymbol{\alpha}} \Psi_{\boldsymbol{\alpha}}\right] = \sum_{\boldsymbol{\alpha} \in \mathcal{A}\setminus\mathbf{0}} d^2_{\boldsymbol{\alpha}} \|\Psi_{\boldsymbol{\alpha}}\|^2. \tag{8}$$

In the last summation, the index $\mathbf{0}$ is removed from the set $\mathcal{A}$ because it corresponds to the mean of the expansion. The mean and variance of the y-coordinate of the model response are obtained similarly. The covariance $R_{\hat{x}\hat{y}}$ can be derived using the orthogonality of the polynomials of the basis, leading to:

$$R_{\hat{x}\hat{y}} = \sum_{\boldsymbol{\alpha} \in \mathcal{A}\setminus\mathbf{0}} d_{\boldsymbol{\alpha}} e_{\boldsymbol{\alpha}} \|\Psi_{\boldsymbol{\alpha}}\|^2. \tag{9}$$

Then, the covariance matrix Σ is constructed from (8) and (9):

$$\Sigma = \begin{bmatrix} \sigma^2_{\hat{x}} & R_{\hat{x}\hat{y}} \\ R_{\hat{y}\hat{x}} & \sigma^2_{\hat{y}} \end{bmatrix}. \tag{10}$$

The covariance matrix Σ can then be used to draw confidence regions, as detailed in [4].

It was demonstrated in [11] that the Sobol' sensitivity indices can be obtained from the expansion coefficients in (5) and (6). These sensitivity indices translate how each of the input variables of the problem contributes to the output uncertainty. In this case, a large Sobol' index corresponding to one anchor means that this anchor contributes a lot to the uncertainty on the position. In this work, we limit ourselves to the use of the total Sobol' sensitivity indices, which for anchor i is given for the x-coordinate by:

$$ST_i^{(x)} = \sum_{\boldsymbol{\alpha} \in \mathcal{J}_i} d^2_{\boldsymbol{\alpha}} \|\Psi_{\boldsymbol{\alpha}}\|^2 / \sigma^2_{\hat{x}}. \tag{11}$$

In this equation, the set $\mathcal{J}_i$ includes all multi-indices $\boldsymbol{\alpha}$ whose i-th component is non-zero. In other words, the square of all coefficients that are related to angle θ_i measured by anchor i are summed and then normalized by the total variance. $ST_i^{(x)}$ therefore represents the proportion of the total variance of the x-coordinate that is effectively due to the anchor i.

C. Anchor selection using Polynomial Chaos Expansions

Our method starts by collecting the AoA measurements and associated uncertainties at the anchors. The Polynomial Chaos Expansion of the x and y-coordinates are then computed. The estimated position is given by (7) and the confidence region is derived from the covariance matrix (10). The total sensitivity indices are computed with (11) for the x and y coordinates separately. For each anchor, both sensitivity indices are then summed $ST_i = ST_i^{(x)} + ST_i^{(y)}$. The anchor corresponding to the highest value of ST_i is then eliminated, and new expansions are computed using the $N-1$ other anchors. This method can be applied iteratively, eliminating one anchor from the set at each step.

III. Experimental setup

A. Setup geometry

An experimental setup was built to validate our method. Six anchors were assembled and connected to a central computer. Each anchor was built using a USRP X310 equipped with 2 UBX daughterboards, and an antenna array, as can be seen in Fig. 2. From this 2-by-2 array, we only used two antennas horizontally spaced by 6 cm, because we aim to localize in two dimensions and therefore we only need to estimate the azimuth angle. The over-the-air calibration procedure at the anchors was realized in the following way. A continuous narrowband signal at 2.5 GHz carrier frequency was generated by a USRP b205mini-i. This signal was distributed to the center pin of each antenna array using power splitters and coaxial cables. Each anchor then recorded a large series of samples on both its channels. The phase difference between the two channels was then computed and stored as reference for calibration. This calibration accounts for all hardware contributions at once, and experiment showed that it is stable in time.

The emitter consists of a USRP b205mini-i connected to a monopole antenna on a movable stand, sending a continuous wave signal at 2.5 GHz carrier frequency. The antennas at the anchors were therefore spaced by one half-wavelength.

Fig. 3 shows the 6 anchors installed on a large table. As the anchors were placed by hand, we took into account an uncertainty on the orientation of each anchor of 2°. All measurements were voluntarily performed with a high gain at the emitter to ensure a high signal-to-noise ratio (SNR) on the received samples. A typical value of SNR observed at the receiver is 45 dB. This allowed us to add noise during the treatment of the data in order to reach the desired SNR at each anchor.

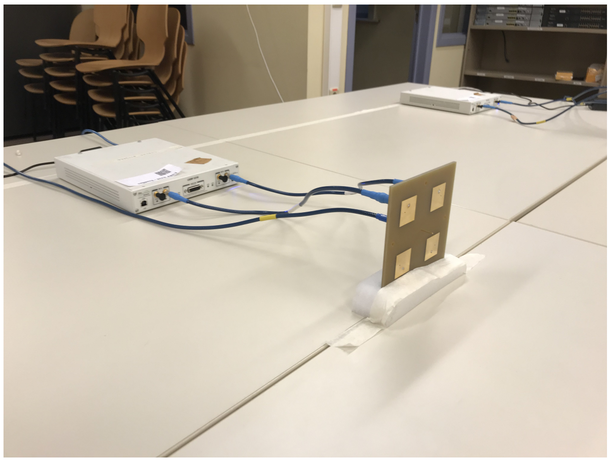

Fig. 2. Picture of one anchor. Two antennas of the array are used.

Fig. 3. The full setup consists of 6 independent anchors, all connected to a central computer. The emitter antenna is a 2.4GHz monopole mounted on a movable stand.

B. Measurement noise addition

Additive white Gaussian noise was added directly on the received samples with the power corresponding to the desired SNR. This measurement noise can be translated into an uncertainty on the AoA using the Cramér-Rao lower bound (CRLB). It is demonstrated in [12] that the CRLB for AoA estimation by an uniform linear array of M antennas is given by:

$$\sigma_\theta^2 \geq \frac{12}{M(M^2-1)} \left(\frac{\lambda}{2\pi d \cos\theta}\right)^2 \frac{\mathrm{SNR}^{-1}}{L} \tag{12}$$

where L is the number of samples, λ is the carrier wavelength, d is the inter-antenna spacing and θ is the AoA measured from broadside. Since our PCE-based method requires a measure of the uncertainty on the AoA as input, the latter was estimated with the CRLB (12) using the SNR of the received signal and the AoA θ estimated with MUSIC [10]. To that result, we added the orientation uncertainty of 2° defined by expert judgement.

TABLE I
SNR AND TOTAL SENSITIVITY INDICES AT EACH ANCHOR IN THE FIRST EXAMPLE

Anchor	1	2	3	4	5	6
$x[m]$	1	2.8	3.7	1	1.7	3.7
$y[m]$	0.5	2.6	0.5	1.9	2.6	1.9
SNR [dB]	8	5	5	5	5	5
$ST^{(x)}$	0.28	0.13	0.35	0.07	0.11	0.08
$ST^{(y)}$	0.27	0.00	0.05	0.30	0.33	0.05
ST	0.55	0.13	0.40	0.37	0.43	0.13

IV. RESULTS

The experimental setup was used as follows. The anchors were placed at known positions, surrounding the large table. The emitter antenna was also placed at a known position in order to evaluate the estimation error of the proposed localization method. Large sets of samples were recorded at each anchor for several positions of the emitter. However, the results presented hereunder all used 10 samples per measurement at each antenna. Note that all distances are given in meters.

A. Example of confidence regions and selection

The first result is an example of the proposed localization method. The emitter was placed at position $(3, 1.3)$. The six anchors recorded 10 samples at each antenna. The AWGN was added on each sample, with power corresponding to the SNR given in Table I for each anchor. The AoA's were estimated using MUSIC algorithm. Then (12) was used to estimate the AoA estimation uncertainty to which was added the 2° orientation uncertainty. The PCE of the position coordinates were computed as (5) and (6) using UQLab [13], [14]. A third degree expansion was chosen and an Ordinary Least Squares regression scheme was used to compute the coefficients. The estimated position is given by the mean of the expansions (7). The covariance matrix (10) was used to draw the 90% confidence region around the estimated position. The total sensitivity indices derived from the PCE are given in Table I.

Although anchor 1 exhibits the highest SNR, our method selects it to be discarded as its total sensitivity index ST is the highest. The PCE-based positioning is then repeated with the five remaining anchors, producing another estimated position and associated confidence region. These results are shown in Fig. 4. A significant amelioration of the estimation is observed when the anchor with the highest ST is discarded. This example is interesting because the anchor that was eliminated from the set was subject to the highest SNR. It was therefore not trivial to select that particular anchor to be eliminated. Hence the proposed PCE-based anchor selection method is able to select the best anchor subset considering the entire problem, even in situations where the best subset would be counter-intuitive.

B. Performance of the proposed method in equal noise conditions

To evaluate the performance of the proposed method, we applied it on 500 measurements and noise realizations, with all other parameters unchanged. The geometry given in Table I was used, and we kept 10 measured samples per antenna. The PCE-based anchor selection method was applied iteratively until only two anchors were remaining. Hence for each noise realization, we obtain 5 estimations of the position: using 6, 5, 4, 3 and 2 anchors. The SNR imposed at each anchor was 10 dB in the first calculation. The cumulative distribution function (CDF) of the positioning error is given in Fig. 5. The probability of reduction P_{red} is defined as the probability that the positioning error is lower with $N-1$ anchors than with N. The root mean square error (RMSE), the median error, as well as probability of reduction are given in Table II. The second calculation was similar to the latter except that a SNR of 5 dB was applied to every anchor. The CDF's obtained for that calculation are given in Fig. 6 and the statistical values in Table III.

In both examples, the precision of localization increases as the first highest ST anchors are eliminated. The precision gain is considerable when 5 anchors out of 6 are selected.

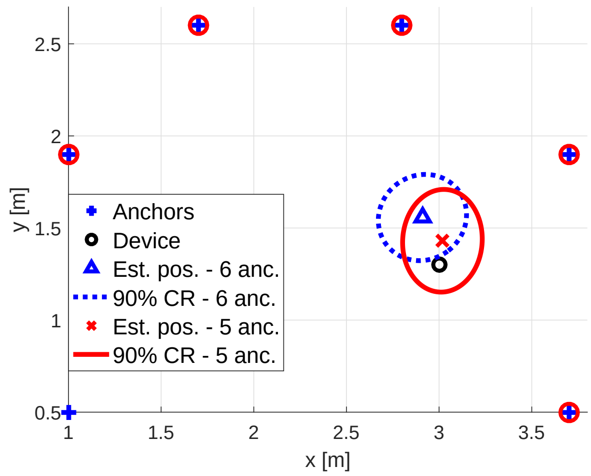

Fig. 4. Anchor locations, position estimates and associated 90% confidence regions before and after anchor selection using the Sobol sensitivity indices. The blue crosses, triangle and dotted ellipse show the 6-anchor situation, while the red circles, cross and continuous ellipse show the selected 5-anchor situation.

TABLE II
RMSE, MEDIAN ERROR AND PROBABILITY OF REDUCTION. SNR = 10 dB

Number of anchors	6	5	4	3	2
RMSE $[m]$	0.18	0.13	0.10	0.12	5.72
Median error $[m]$	0.17	0.11	0.09	0.09	0.13
$P_{red}[\%]$	93	62	45	34	/

TABLE III
RMSE, MEDIAN ERROR AND PROBABILITY OF REDUCTION. SNR = 5 dB

Number of anchors	6	5	4	3	2
RMSE $[m]$	0.24	0.18	0.18	0.24	22.7
Median error $[m]$	0.21	0.14	0.13	0.14	0.27
$P_{red}[\%]$	77	57	43	27	/

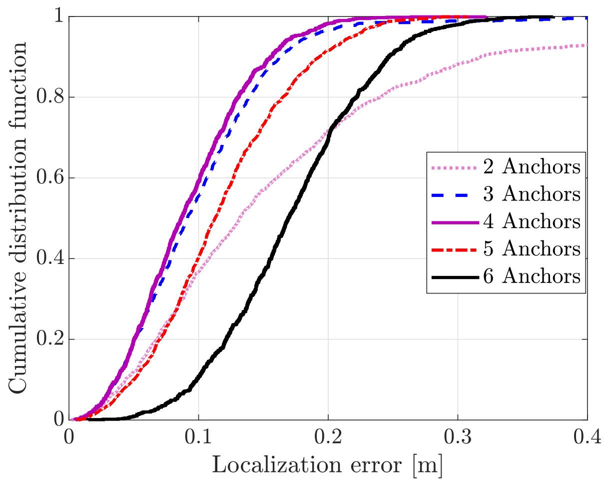

Fig. 5. Cumulative distribution function of the localization error. Comparison of the localization performance using 6, 5, 4, 3 or 2 anchors (SNR = 10 dB).

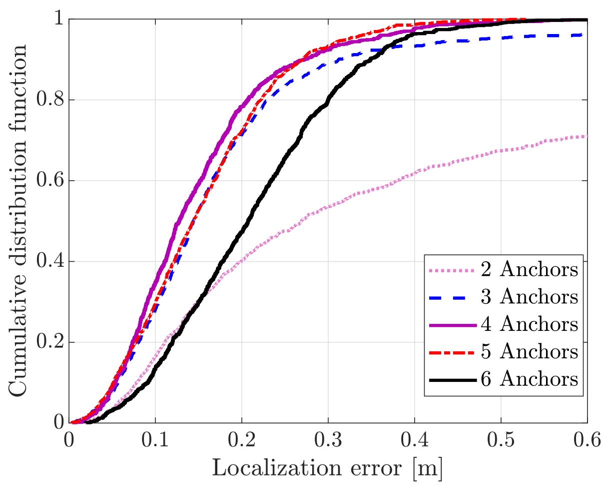

Fig. 6. Cumulative distribution function of the localization error. Comparison of the localization performance using 6, 5, 4, 3 or 2 anchors (SNR = 5 dB).

However, once a set of four anchors is selected, further selection to form 3- or 2-anchors subsets cause a decrease of the localization precision. It is observed in both examples that P_{red} decreases as the number of anchors decreases. In fact, a link can be made between P_{red} and the precision gain: when discarding an anchor, the precision of localization increases when $P_{red} > 50\%$. Indeed, in both examples, P_{red} drops under 50% when 4 anchors remain from the selection process. The RMSE and median error also reach a minimum value with 4 anchors. In the 10 dB example, the localization error using the selected 4 anchors is under 15 cm with probability 88%, while using the using 6 anchors without selection this probability is 36%. We can infer that our method can considerably improve the precision of localization. Nevertheless, there is an optimal number of anchors to discard in order to obtain the best localization performance.

V. Conclusion

To enhance the localization performance of angle-of-arrival estimation-based positioning systems, we proposed an anchor selection method using Polynomial Chaos Expansions. The selection is based on the total sensitivity indices derived from the PCE, which express the fraction of positioning uncertainty that is due to each anchor. An experimental setup was used to collect measurement data on which the method was applied. Results show that the method can effectively select the best anchor subset considering the whole system and not simply eliminate the anchor with the highest SNR. A performance study showed that the localization precision is considerably improved when the proposed selection method is applied on a 6-anchors set in equal noise situations.

Acknowledgements

The authors would like to express their gratitude to the ICTEAM department of the Université Catholique de Louvain for providing the antenna arrays. The authors would also like to thank the F.R.S-FNRS and Innoviris through the Copine-IoT project for financial support.

References

[1] X. Lin, J. Bergman, F. Gunnarsson, O. Liberg, S. Razavi, H. Razaghi, H. Rydn, Y. Sui, *Positioning for the internet of things: A 3GPP perspective*, IEEE Communications Magazine, vol. 55, no. 12, pp. 179-185, 2017

[2] K. Witrisal, C. Anton-Haro, *Whitepaper on New Localization Methods for 5G Wireless Systems and the Internet-of-Things*, http://www.iracon.org/wp-content/uploads/2018/03/IRACON-WP2.pdf, COST ACTION CA15104, 2018

[3] T. Van der Vorst, M. Van Eeckhaute, A. Benlarbi-Delai, J. Sarrazin, F. Quitin, F. Horlin, P. De Doncker, *Angle-of-Arrival based localization using polynomial chaos expansions*, Proc. of the Workshop on Dependable Wireless Communications and Localization for the IoT, 2017

[4] T. Van der Vorst, et al., *Application of Polynomial Chaos Expansions for Uncertainty Estimation in Angle-of-Arrival Based Localization*. In : Uncertainty Modeling for Engineering Applications. Springer, Cham, 2019. p. 103-117.

[5] L. Kaplan, *Local node selection for localization in a distributed sensor network*. IEEE Transactions on Aerospace and Electronic Systems, 42(1), 136-146, 2006.

[6] Q. Yan, J. Chen, L. De Strycker, *An Outlier Detection Method Based on Mahalanobis Distance for Source Localization*. Sensors, 2018, vol. 18, no 7, p. 2186.

[7] Q. Yan, J. Chen, G. Ottoy, L. De Strycker, *Robust AOA based acoustic source localization method with unreliable measurements*. Signal Processing, 152, 13-21, 2018.

[8] R. Zekavat, R. Buehrer, *Handbook of position location: Theory, practice and advances*, John Wiley & Sons, 2011.

[9] C. Godara, *Application of antenna arrays to mobile communications. II. Beam-forming and direction-of-arrival considerations*, Proceedings of the IEEE, 1997, vol. 85, no 8, p. 1195-1245.

[10] R. Schmidt, *Multiple Emitter Location and Signal Parameter Estimation*, IEEE Transactions on Antennas and Propagation, 34, pp 276-280, 1986.

[11] B. Sudret, *Global Sensitivity Analysis Using Polynomial Chaos Expansions*, Reliab. Eng. Sys. Saf., 93, pp 964-979, 2008.

[12] S. Kay, *Fundamentals of statistical signal processing*, Prentice Hall PTR,1993.

[13] S. Marelli, B. Sudret, *UQLab user manual - Polynomial Chaos Expansions*, Chair of Risk, Safety & Uncertainty Quantification, ETH Zurich, 2015.

[14] S. Marelli, C. Lamas, B. Sudret, et al. *Uqlab user manual–sensitivity analysis*. Tech. Rep, 2015.